The Mechanism Behind the Oxidation Protection of High Mg Al Alloys with Beryllium

NICHOLAS SMITH, ANNE KVITHYLD, and GABRIELLA TRANELL

The addition of beryllium to Al-Mg alloys is known to cause a dramatic decrease in oxidation; however, the mechanism behind this protective effect is not yet fully understood. To aid in finding an alternative to the toxic Be, a fundamental study of Be additions has been carried out. Industrial samples containing 2 ppm Be and a model alloy with 100 ppm Be were oxidized at temperatures between 550 °C and 750 °C in a horizontal tube furnace. The oxide layer and oxide–metal interface were investigated using SEM, FIB, and XPS. It was found that Be forms a uniform oxide layer at the oxide–metal interface which slows the diffusion of Mg and Al from the metal into the oxide layer resulting in a reduced oxidation rate and an increase in the time for breakaway oxidation to occur.

I. INTRODUCTION

BERYLLIUM additions in ppm levels have long been used by the aluminum industry as a means of reducing the excessive oxidation that can occur when producing Al alloys with an elevated Mg content. Through TGA experiments, the effects of Be were well documented by Balicki already in 1958, Thiele in 1960, and Cochran in 1976.[1–3] The benefits of Be additions come in reducing the total amount of oxidation over short timeframes, as well as increasing the time until the onset of breakaway oxidation. However, owing to the limited ability of many quantification techniques to detect trace amounts of Be, the mechanism by which Be influences the oxidation has not been fully understood. Due to the significant health risks posed by Be and BeO, especially to the workers in the aluminum casthouses, the use of Be is restricted, and alternative methods are preferred.[4]

The addition of Mg to an Al alloy causes an MgO oxide layer to form, which is further transformed to $MgAl_2O_4$; once all the Mg is oxidized from the melt, these oxides are considered nonprotective in terms of preventing further oxidation. Mg-containing alloys will initially oxidize at a low rate; however, after a period of time ranging from minutes to hours, there will be a sudden and sharp increase in the oxidation rate, known as breakaway oxidation that will continue until all the Mg in the melt is oxidized. The oxidation will result in a notable loss of Mg from the melt. Therefore, extra steps are generally required when producing alloys with a high Mg content to minimize the oxidation. Ppm level additions of Be have been shown to reduce both the amount of oxidation and delay the onset of breakaway oxidation. This results in a reduction of the amount of Mg lost to oxidation and a reduction in the number of oxide inclusions that enter the melt during casting.[1–3,5] The focus of this study will be on describing the formation of the oxide layer in the presence of Be during the incubation period of oxide growth, rather than breakaway oxidation, as the former is the most important time period with respect to industrial Al production—as the primary aim of oxidation control in the casthouse is to remain in the incubation stage and avoid catastrophic breakaway oxidation.

To better understand the mechanism behind how trace Be additions can result in a marked drop in the oxidation of Al-Mg alloys, a series of experiments were undertaken to characterize the oxide layer and the effects of Be on the layer.

II. EXPERIMENTAL

The primary experimental study focused on oxidation experiments conducted in a horizontal tube furnace; however, supplementary metal–oxide reaction and oxide-stability experiments were carried out to support the findings.

A. Oxidation Experiments

Figure 1 shows one of the two horizontal tube furnaces and the sample loading system utilized to carry out the oxidation experiments. Ground (22 μm) or polished (1 μm) flat samples measuring approximately

NICHOLAS SMITH and GABRIELLA TRANELL are with the NTNU, Alfred Getz Vei 2, 7034 Trondheim, Norway. Contact e-mail: nicholas.smith@ntnu.no ANNE KVITHYLD is with the SINTEF, Sluppen, P.O. Box 4760, 7465 Trondheim, Norway.

$25 \times 15 \times 1.5$ mm were placed in an alumina boat suspended in the furnace and held for a set time and temperature under an air atmosphere in the furnace as shown in Figure 1. This method gives samples that can be analyzed from various oxidation times, showing how the oxide morphology evolves with time. The samples were removed from the furnace after the required holding time and analyzed by means of a scanning electron microscope (SEM), dual-beam focused ion beam miller (FIB), and X-ray photoelectron spectroscopy (XPS). Table I shows the experimental matrix for the experiments done in the tube furnace.
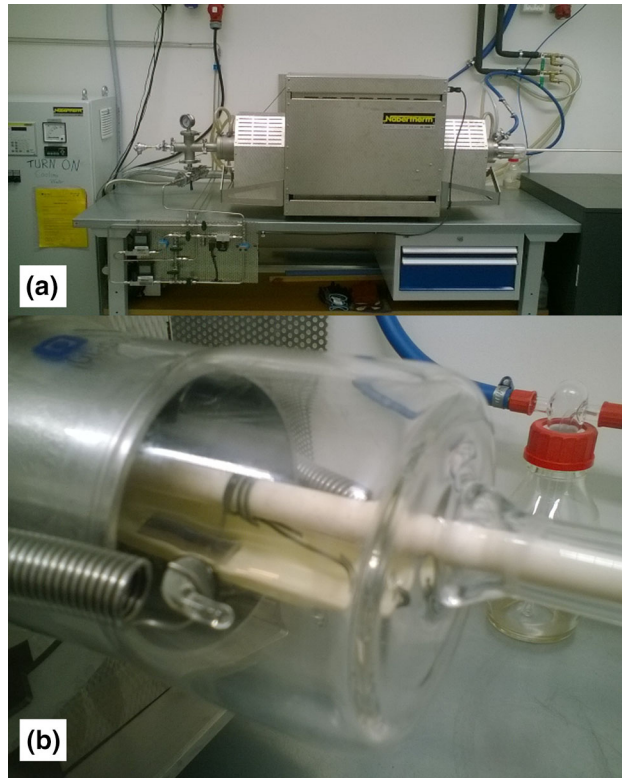

Fig. 1—(*a*) Horizontal tube furnace used for oxidation tests of 100 ppm Be samples. (*b*) Sample loading system for the horizontal tube furnace with sample in alumina boat.

The first series of experiments were carried out on industrially produced 5XXX series Al alloys. Two different alloys were used: one containing 2 ppm of Be and the other being Be free. Besides the Be content, both alloys were of the same grade and had a similar Mg content (4.7 pct). Samples were cut with a SiC abrasive saw and ground to 22 μm with SiC paper on all sides. To minimize oxidation at room temperature, the sample was placed in the furnace within 30 minutes of the final grinding. Samples were held at temperatures between 550 °C and 750 °C for 10, 30, or 120 minutes with the mass of each sample measured before and after oxidation to find the percentage mass gain due to oxidation.

To enhance the effects of Be, a second set of experiments was carried out on a model alloy with an elevated Be content over what is typically found in industrial alloys; this alloy consisted of 100 ppm of Be and 4.5 pct Mg in pure Al. It was assumed that the higher level of Be would only act to enhance the effects and aid in the detection of Be without changing the overall oxidation protection mechanism. The alloy was made from 99.999 pct pure Al from Puratronic, 99.98 pct pure Mg from Sigma Aldrich, and 99 pct pure Be from Alfa Aesar. First, a 0.5 pct AlBe master alloy was made in an arc melter that passed an electrical current through a tungsten electrode, creating an arc that rapidly melted the metal. The sample was then rapidly cooled on a water-cooled copper plate. This process was repeated several times to ensure a homogeneous alloy. The master alloy plus Al and Mg was charged into an alumina crucible and heated in an induction furnace to 850 °C and held for 15 minutes. It was then sectioned to size, polished to a 1 μm finish using a SiC abrasive saw and standard sample polishing techniques, to allow generation of the best possible chemical composition and depth profile.

B. Sample Analysis

A FEI Helios NanoLab DualBeam FIB was used to examine the surface of the samples after oxidation. After examination of the surface, the gallium ion beam was used to cut vertically down through the surface of the oxide and into the bulk metal. This allows a cross section of the oxide layer to be examined and the thickness of the layer to be measured.

Table I.   Experimental Matrix for Oxidation Experiments of an Al 4.5 Pct Mg Alloy Containing Beryllium

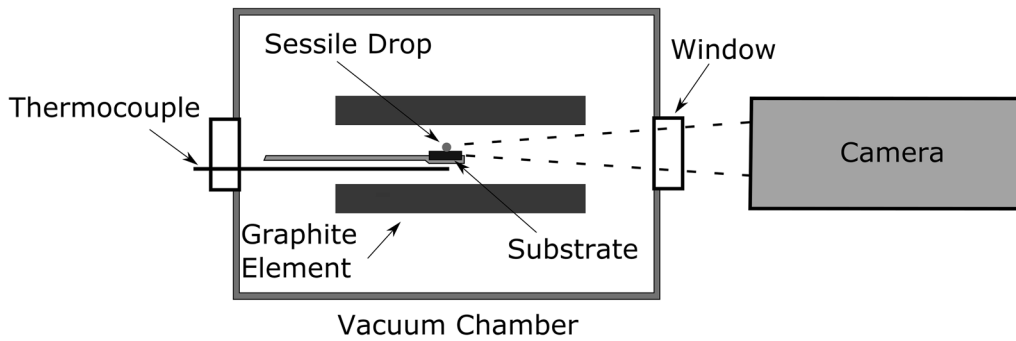| Temp (°C)	Time (Min)						
	10	30	45	60	90	120	360
2 ppm Be							
550	X	X				X	
700	X	X				X	
750	X	X				X	
100 ppm Be							
550		X	X	X	X		X
700							X
750		X		X		X	

Fig. 2—Sessile drop furnace setup used to study the reaction and contact angle between oxide substrates and AlBe alloys under a high vacuum at 1100 °C.
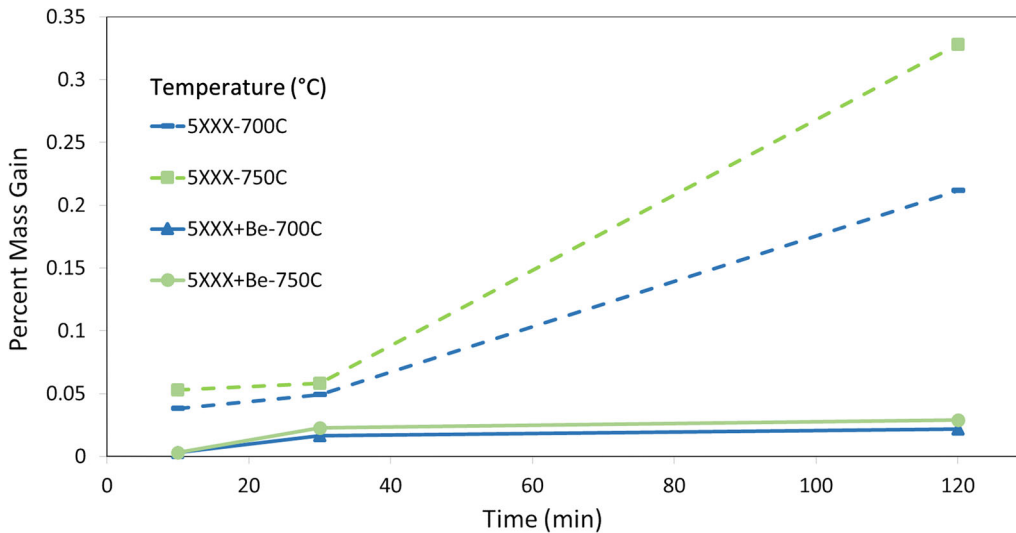

Fig. 3—Percentage mass gains in samples with and without 2 ppm Be oxidized in synthetic air for 10, 30, or 120 min at 700 °C and 750 °C showing a significant decrease in the total amount of oxidation with the addition of 2 ppm Be.

A Thermofisher Thetaprobe XP Spectrometer was used to create a XPS composition depth profile from the top surface through the oxide layer into the base metal. To create the depth profile, argon sputtering was used with an estimated sputtering rate of 8 nm per analysis cycle (120 seconds of sputtering time).

C. Metal–Oxide Reaction

The effects of Be on an Al drop in contact with Al_2O_3 and MgO substrates was measured using a sessile drop furnace as seen in Figure 2. This setup allowed observation of any reactions between the metal and substrate, as well as measuring the metal–substrate contact angle.

Pure Al with 0, 30, or 60 ppm of Be was tested on both Al_2O_3 and MgO substrates. In order to test the contact angle between the metal droplet and the substrate without interference of the oxide skin on the Al drop, the oxide skin was removed under a high vacuum/low oxygen partial pressure. Under a high vacuum, the Al_2O_3 skin will become less stable, and

there is a decrease in thickness of the skin as the flux of oxygen away as AlO gas will exceed the flux of oxygen into the skin. The rate of this evaporation is temperature dependent, and, at temperatures over 1100 °C, the oxide skin can be completely removed in a short time.[6] Once the skin has been removed, a stable contact angle can be measured. In the experiments, the samples were held for two hours under a 1.5×10^{-5} mbar vacuum at 1100 °C.

D. Oxide Stability

Experiments to better understand the stabilities of BeO, MgO, and Al_2O_3 when mixed were carried out by mixing these three oxides in powder form in a 1:1:1 and a 1:1:2 ratio ($BeO:MgO:Al_2O_3$) and placed in Mo crucible and held at 1100 °C for 7 hours. The samples were subsequently analyzed using a D8 Focus powder X-ray Diffractometer (XRD) to see which phases had formed. The XRD scan was completed with a two theta angle ranging from 15 to 105 deg. This range captured all the major known peaks associated with the ternary BeO-MgO-Al_2O_3 system.
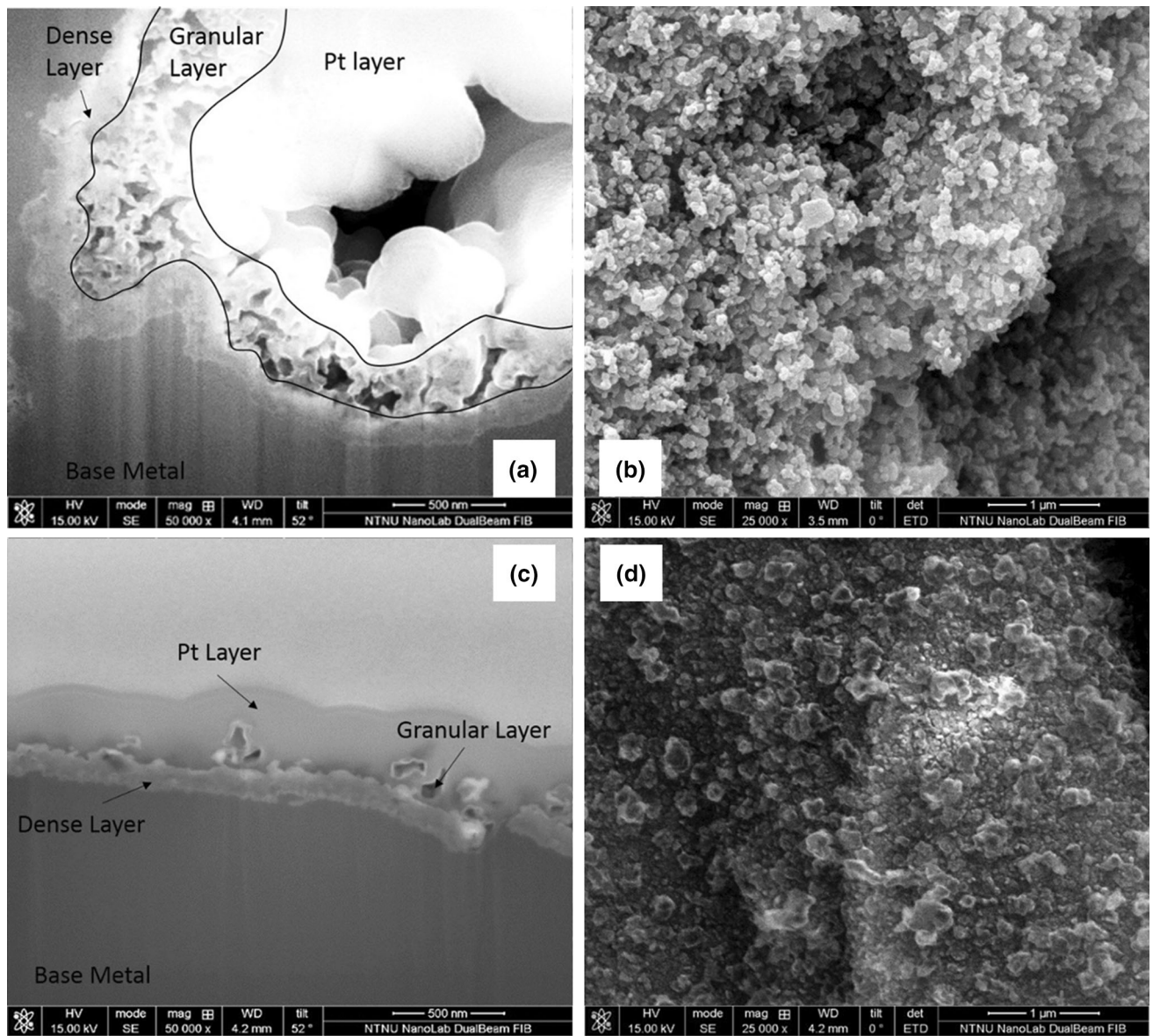
Fig. 4—Samples from oxidation experiments in synthetic air in the horizontal tube furnace shown in (*a*). Cross section of sample without Be from 120 min at 700 °C showing large amounts of granular growth on the top of the oxide layer. (*b*) Top surface of sample without Be from 120 min at 700 °C with granular growth covering the entire sample surface. (*c*) Cross section of sample with 2 ppm Be from 120 min at 700 °C with only minor granular growth being visible. (*d*) Surface of sample with 2 ppm Be from 120 min at 700 °C showing only minimal coverage of the granular layer.

III. RESULTS

A. *Beryllium in Industrial Al-Mg-Be Samples*

1. *Mass gain*

The addition of 2 ppm of Be was found to have a significant impact on the total amount of oxidation/sample mass gain. Figure 3 shows the percentage mass gain of the samples with and without 2 ppm Be. The addition of Be resulted in up to a tenfold decrease in the mass gain.[7] These results are in agreement with previous mass gain and TGA analysis conducted on Be in Mg-Al alloys.[1–3]

2. *Surface and cross-sectional morphology*

The addition of Be had a clear impact on the morphology of the oxide layer. Figures 4(a) through (d) shows the top surface and cross section of samples oxidized at 700 °C. In Figures 4(a) and (b), two distinct oxide layers can be seen on the sample without Be: a dense layer adjacent to the metal, and a granular layer on top of the dense layer. The platinum layer above the granular layer in the cross-section figures was deposited by the FIB during the process of making the cross section to protect the integrity of the granular layer from the ion beam. With the addition of Be, the thickness of
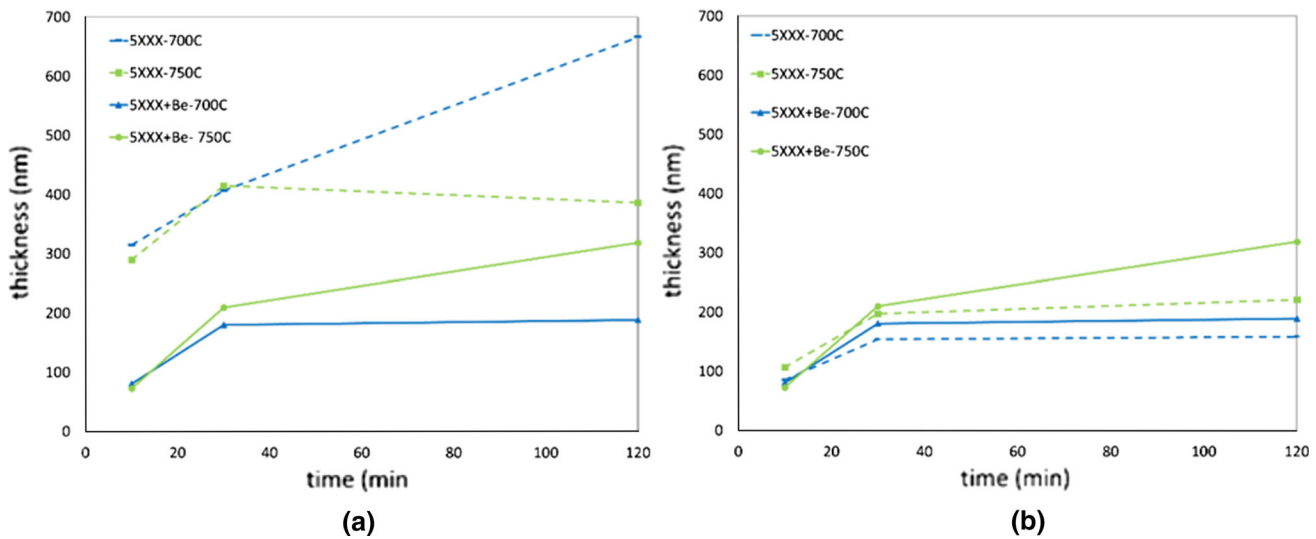
Fig. 5—Measured oxide layer thicknesses of samples oxidized in air at 700 °C and 750 °C. (*a*) The thickness of the entire oxide layer. (*b*) The thickness of only the dense oxide layer.
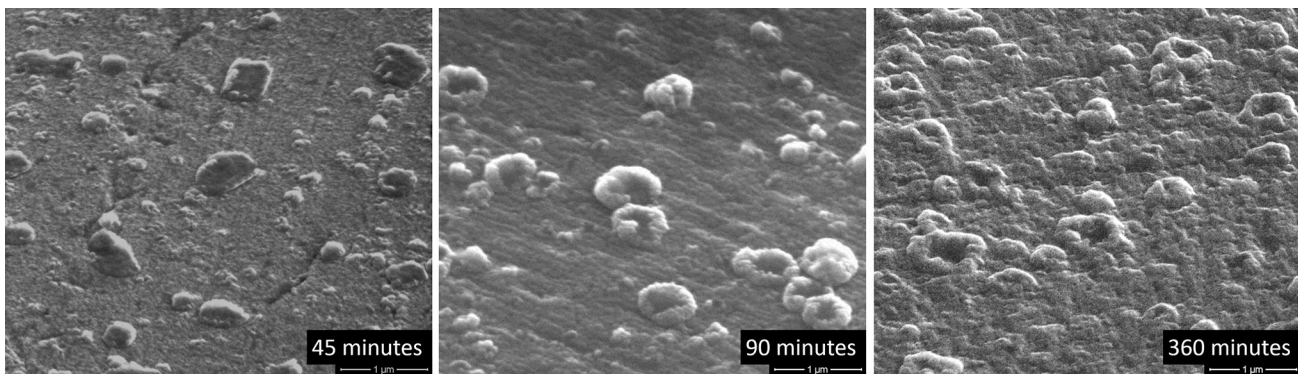

Fig. 6—FIB images from 45, 90, and 360 min of oxidation in air at 550 °C on sample with 100 ppm Be, showing the rapid formation of growths on the surface and envelopment of the growths by the surrounding oxide layer with time.

the granular layer is significantly reduced as can be seen in Figures 4(c) and (d) where the amount of granular layer can be seen to be reduced to near zero, whereas the dense layer has a nearly consistent thickness between the two alloys. The granular layer is made up of many small, often faceted granules that grow out of the dense oxide layer creating an open network of oxide.[7] This layer is similar in appearance to MgO oxide layer found by other researchers on Al-Mg alloys.[3,8,9]

Figure 5(a) shows the thickness of the entire oxide layer measured from the FIB cross sections. Exact measurement of the granular layer thickness was not possible due to the uneven nature of the layer, and therefore, the thickness of this layer should be taken as an indication of the approximate thickness, not the exact thickness. Figure 5(b) shows the thickness of just the dense layer. A comparison of the thickness of the oxide layers shows that the thickness of the dense layer is similar between the samples with and without Be.[7] The significant difference between the Be-containing and Be-free alloys is the granular layer thickness.

B. Model 100 ppm Al-Mg-Be Samples

1. Surface and cross-sectional morphology

Examination in the FIB of samples with 100 ppm Be oxidized at 550 °C for 45, 90, and 360 minutes showed that within the first 45 minutes, the surface of the sample was covered in growths measuring up to 0.5 μm across. These growths appeared to remain nearly constant in size for longer oxidation times, as illustrated by Figure 6. The oxide surrounding these growths was seen to grow and began to envelop the growths after 360 minutes of oxidation time. These growths are not present on a reference sample that was oxidized under the same conditions, but contained no Be as shown in Figure 7; rather the surface was covered in large granular MgO growths.[10]

The formation of the growths was not uniform across the entire sample surface with the number of growths varying from region to region. Grain boundaries particularly appeared to be nucleation sites for the growths as seen in Figure 8.[10]
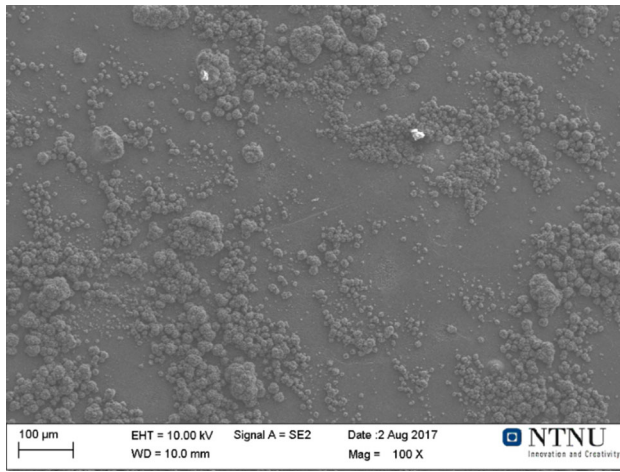
Fig. 7—Surface of reference sample without Be oxidized for 240 min at 550 °C in air showing the large granular MgO growths on the surface, but no smaller, dense growths, as seen on the Be-containing sample (Fig. 6).
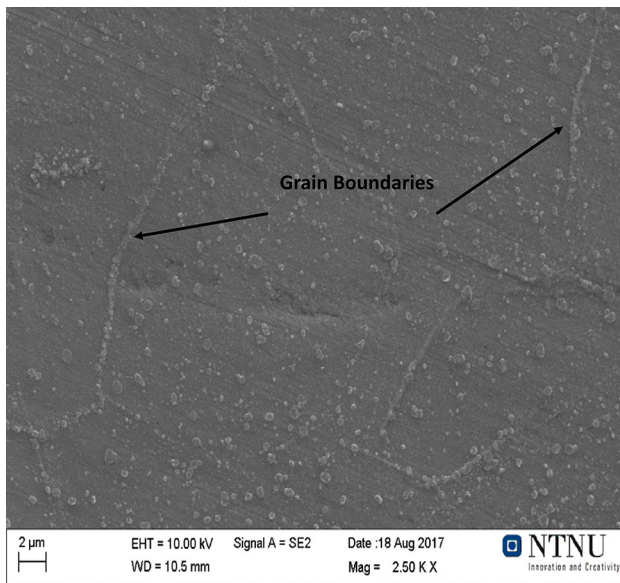

Fig. 8—100 ppm Be sample oxidized for 360 min at 550 °C in air showing preferential growth along the grain boundaries.

2. Composition

Samples for the XPS were sectioned from the 100 ppm sample oxidized at 550 °C for 60 and 360 minutes. The results of the XPS are given in Figures 9 and 10.[10] In these figures, an increase in sputtering time indicates an increase in depth taking the top surface of the oxide to be the top and moving downward towards the bulk aluminum metal. Due to the growths that formed on the surface and the uneven sputtering rate that resulted from these growths, it was not possible to accurately calculate depth from sputtering time. A corresponding oxygen ion curve exists for each of the metal oxide curves given in Figures 9 and 10, however, these have been omitted from the figures for simplicity. It can be

seen that for both oxidation times the top surface of the oxide layer is MgO (far left in Figures 9 and 10). Downwards towards the metal the amount of Al oxide increases followed by an increase in the metallic Al concentration. Further downward, a clear BeO signal forms, and the MgO signal decreases to zero. There is little difference between the 60 and 360 minute samples with exception of the thickness of each layer and the ratio of the Be oxide to Al oxide signals. Both XPS curves show that the Mg metal content in the top part of the metal phase is well below the nominal 4.5 pct, indicating a large loss due to oxidation and evaporation.

Figures 11(a) and (b) shows SEM images of the surface of the 360 minute sample before and after sputtering. Before sputtering, the surface can be seen to have the rough granular appearance typical of MgO, but additionally growths on the top surface that are confirmed to be MgO by the XPS, are found. After sputtering for 3000 seconds, two distinct phases appear as seen in Figure 11(b). A bright phase on the surface that corresponds with the location of growths on the surface seen in Figure 11(a) and a darker background phase. An Energy Dispersive X-ray Spectroscopy (EDS) scan showed the bright phase is the only oxygen-containing phase present after sputtering. As the XPS shows the BeO-Al$_2$O$_3$ phase is the only oxygen-containing phase remaining after sputtering, it should correspond with this bright phase, while the dark phase is the Al metal. This is shown schematically in Figure 12 for both the 60 and 360 minute samples.[10]

For the samples oxidized at 700 °C, no large growths were visible on the surface. Rather an uneven surface with a number of small cracks as seen in Figure 13(a). This sample had too much surface topography to allow an XPS analysis. The sample was characterized in the FIB and compared to the 550 °C sample to help understand the means of oxidation protection on molten samples. Figure 13(b) shows a cross section of the 700 °C sample where a thin layer ranging from 15 to 50 nm in thickness exists between MgO oxide layer and bulk metal. Given the location of this layer in comparison with the samples from 550 °C it can logically be assumed that this is a BeO-Al$_2$O$_3$ layer that formed as a uniform layer across the entire oxide metal interface rather than as the clusters seen with oxidation below the melting point.[10]

It is difficult to directly measure the amount of MgAl$_2$O$_4$ and BeAl$_2$O$_4$ phase present from the XPS. It is known that for the MgAl$_2$O$_4$ phase to form the activity of Mg must be below 0.023 which corresponds to 2.7 at. pct and that Al$_2$O$_3$ cannot form until after all MgO has been transformed to MgAl$_2$O$_4$.[5] Therefore, any Al oxide ions found would predominately be associated with the MgAl$_2$O$_4$ or BeAl$_2$O$_4$ spinel phases. The XPS scans clearly show the presence of Al oxide ions indicating that the spinel phase is present. As the Al oxide signal increases before the Be signal, the MgAl$_2$O$_4$ phase is implied. However, at sputtering times over 1600 seconds the Mg oxide ion signal has decreased to zero, but a strong Al oxide signal remains indicating the presence of BeAl$_2$O$_4$. The Al oxide:Be oxide ratio shows
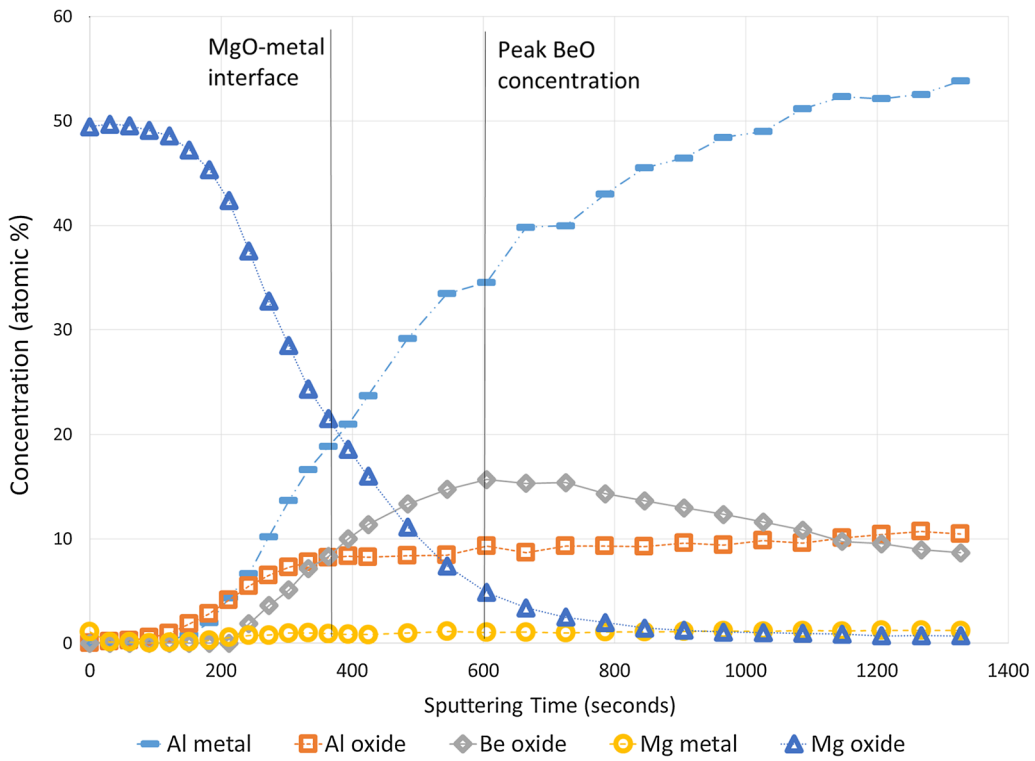
Fig. 9—XPS depth profile of the oxide layer for the sample after 60 min of oxidation time in air at 550 °C.
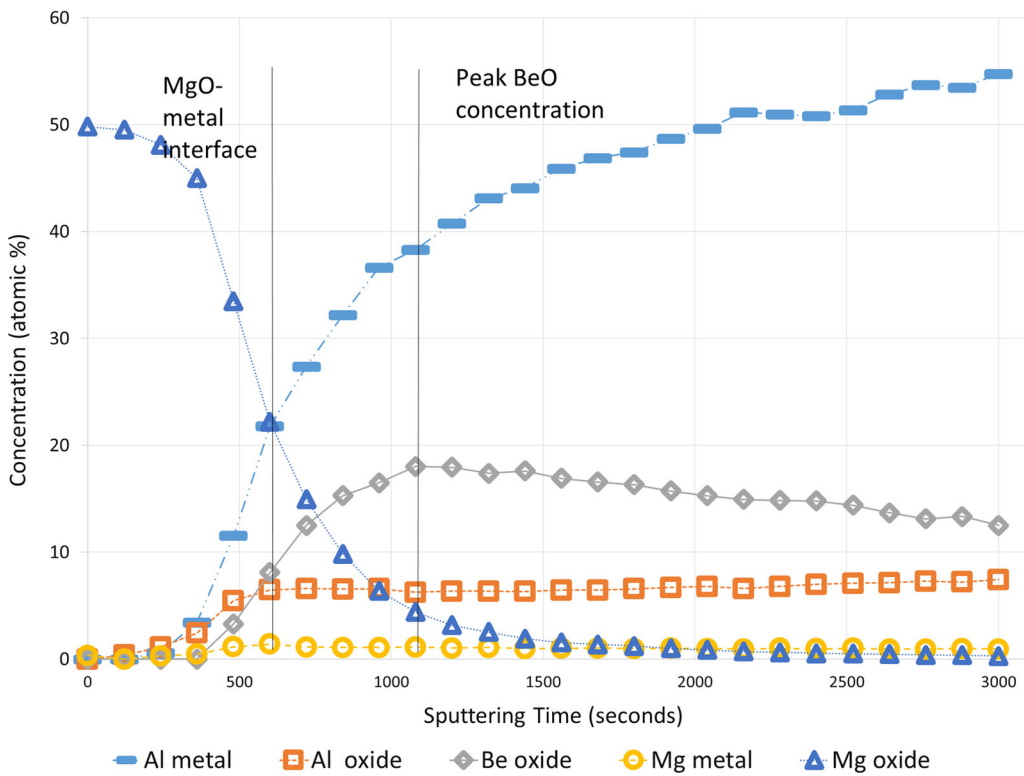

Fig. 10—XPS depth profile of the oxide layer for the sample after 360 min of oxidation time in air at 550 °C.
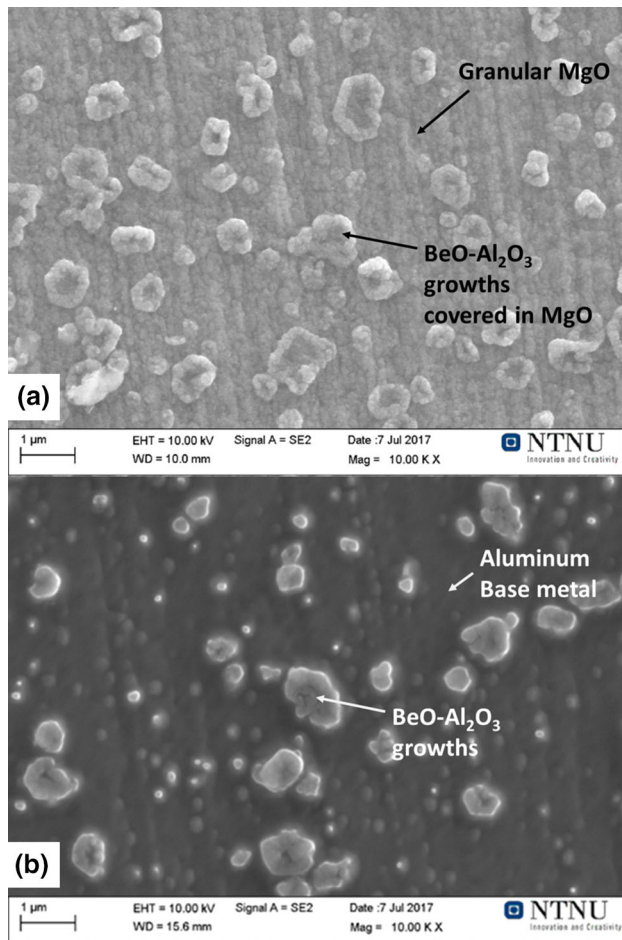
Fig. 11—(a) 100 ppm Be sample oxidized for 360 min at 550 °C before sputtering, showing surface covered by MgO. (b) Same sample only after sputtering/XPS analysis showing 2 distinct phases: a bright oxide phase and a dark metal phase.
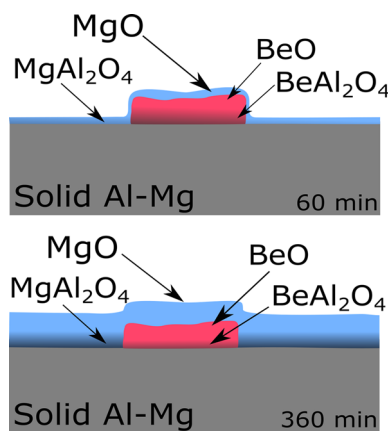

Fig. 12—Schematic showing a cross section of the oxide layer formed on the solid sample after 60 or 360 min of oxidation based on the results of the XPS depth profile and the morphological analysis in the FIB.
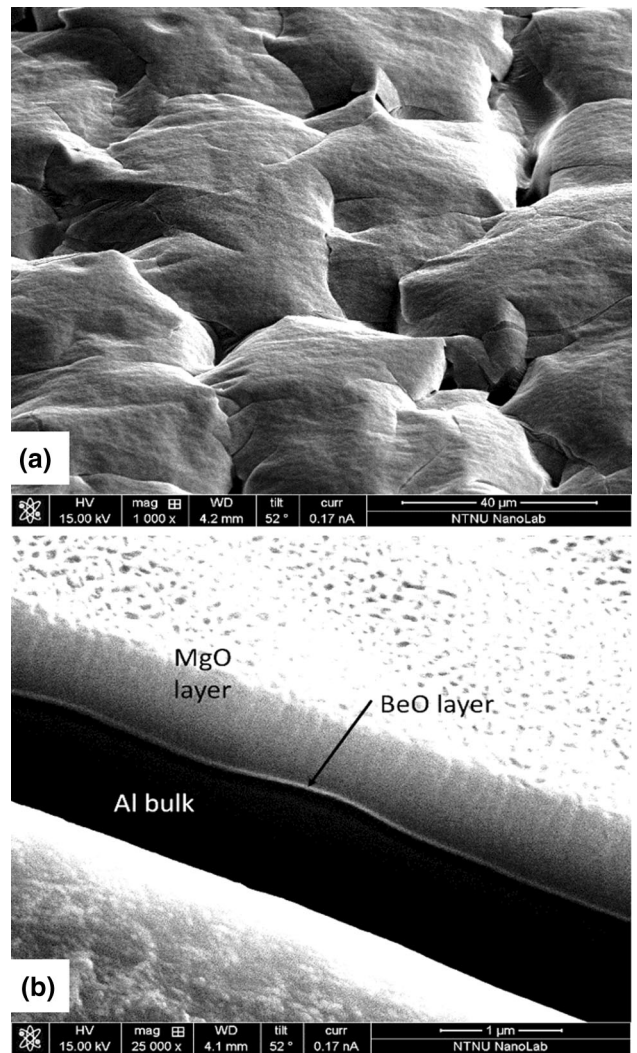

Fig. 13—Sample with 100 ppm Be from 360 min of oxidation at 700 °C in air. (a) Surface showing uneven surface with small cracks. (b) Cross section through oxide layer showing a thin BeO layer that was found between the MgO layer and Al base metal.

that both BeO and $BeAl_2O_4$ must be present after the entire Mg oxide layer has been removed by sputtering as both a Be oxide and an Al oxide signal remain. For the entire layer to be made up of $BeAl_2O_4$, the Al oxide:Be oxide ratio must be 2:1. If the ratio is higher than this, then a $BeAl_2O_4$-Al_2O_3 layer would exist. If the ratio is below 2:1 the layer must be $BeAl_2O_4$-BeO. As the ratio does not reach 2:1 at any point in the depth profile, both BeO and $BeAl_2O_4$ must be present in the oxide layer.

The Al oxide:Be oxide ratio increases as the depth increases for both the 60 and 360 minute oxidation samples with a higher ratio seen for the 60 minute sample which exceeds unity for the last 200 seconds. The higher Al oxide:Be oxide ratio for the shorter oxidation time indicates that the formation of the BeO layer is
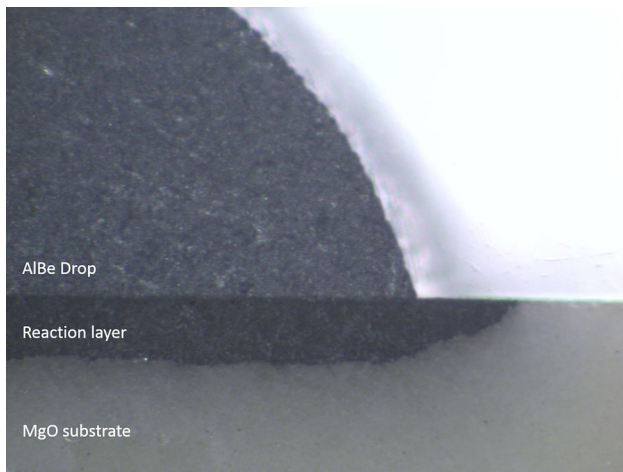
Fig. 14—Sample from Sessile drop furnace showing an Al drop with 60 ppm Be on MgO substrate after holding for 15 min in vacuum at 1100 °C. MgAl$_2$O$_4$ reaction layer between the substrate and drop can be seen.

Table II. Contact Angles Measured on MgO and Al$_2$O$_3$ with 0, 30, or 60 ppm Be in Al

| | Al$_2$O$_3$ | | MgO |
	15 Min	60 Min	15 Min
0 ppm Be	85	54	
30 ppm Be	88	56	77
60 ppm Be	90	62	97

time dependent on the transport of Be from the metal to the oxide layer, with longer times allowing for more concentration and oxidation of Be in the oxide layer. The Al oxide:Be oxide ratio would be further reduced if the oxidation occurs above the melting point as the transport of Be to the oxide–metal interface is faster in the liquid phase.

C. *Metal–Oxide Reaction*

Table II shows the contact angles measured for pure Al with 0, 30 or 60 ppm Be on Al$_2$O$_3$ and MgO substrates for a temperature of 1140 °C. It was not possible to measure the contact angle at times longer than 15 minutes for the samples on the MgO substrate. This is due to the strong reaction of the Al with the substrate. At low pressures, the MgAl$_2$O$_4$ spinel phase is the stable oxide phase. This reaction occurs rapidly resulting in a reaction layer in the substrate and gassing of Mg vapor that is deposited on the furnace walls and windows: this reaction can be written as shown in Eq. [1]. The sessile drop sample with the reaction layer is shown in Figure 14. Due to this reaction the angle measured on the MgO is not stable and is not reliable, but is presented here for thoroughness.

$$4MgO + 2Al = MgAl_2O_4 + 3Mg \qquad [1]$$

D. *Oxide Stability*

An excerpt of the XRD scans for both the 1:1:1 and 1:1:2 mixing ratios are shown together in Figure 15, and were obtained after analysis of the two different oxide powder mixing ratios. The same peaks were seen in both of the scans. The most significant peaks are the oxides BeO, MgO and Al$_2$O$_3$. The major peaks all vary significantly due to the higher Al$_2$O$_3$ content in the 1:1:2 sample. Both BeAl$_2$O$_4$ and MgAl$_2$O$_4$ were found in the samples. A number of overlapping peaks exist for this system, but at least 3 distinct peaks existed for each BeAl$_2$O$_4$ and MgAl$_2$O$_4$. The peaks at 22.15, 27.54 and 56.88 deg are unique to BeAl$_2$O$_4$ and 31.26, 44.79 and 65.78 deg are unique to MgAl$_2$O$_4$.

IV. DISCUSSION

From the morphology studies of the 2 and 100 ppm Be alloys, it can clearly be seen that the growth of the granular layer with time accounts for the bulk of the oxidation occurring on Be-free samples. This oxide growth is rate controlled by the transport of Mg through the dense oxide layer. The effect of Be reducing the granular MgO layer formation is clearly visible on the industrial samples where the thickness of granular layer was reduced to near zero with the addition of 2 ppm of Be. This means the addition of Be must slow the transport of Mg through the oxide layer. This can also be shown by looking at the samples from oxidation at 550 °C (Figure 6) where the oxide layer surrounding the growths increases in thickness faster than the growths—resulting in the growths being enveloped in the MgO. This indicates that the growths inhibit the oxidation. Further, as seen in Figure 7, the oxidation on a Be-free sample at 550 °C occurs at preferential sites resulting in large clusters of MgO. The BeO growths found on the samples containing Be were found at preferential sites such as grain boundaries; it is believed that the BeO growths form at the preferential sites for Mg oxidation resulting in a reduction of the large oxide clusters seen on Be-free samples.

The minor increase in the contact angle seen with increasing amounts of Be, *i.e.* increased wetting is negligible when compared to the error seen with this setup ± 5 deg. The contact angle results for pure aluminum are in good agreement with those found by Bao.[6] Syvertsen carried out measurements of the oxide skin strength on a liquid Al-Mg melt and found that additions of 2 ppm Be had no impact on the skin strength. This offers a confirmation of the wetting results obtained here as the skin strength is partially a measure of the surface tension between the oxide and metal.[11]

The rapid reaction of the Al drop with the MgO substrate shows that even with Be additions MgO will react strongly with liquid aluminum forming the MgAl$_2$O$_4$ spinel unless the MgO layer and Al metal are separated by a protective layer.
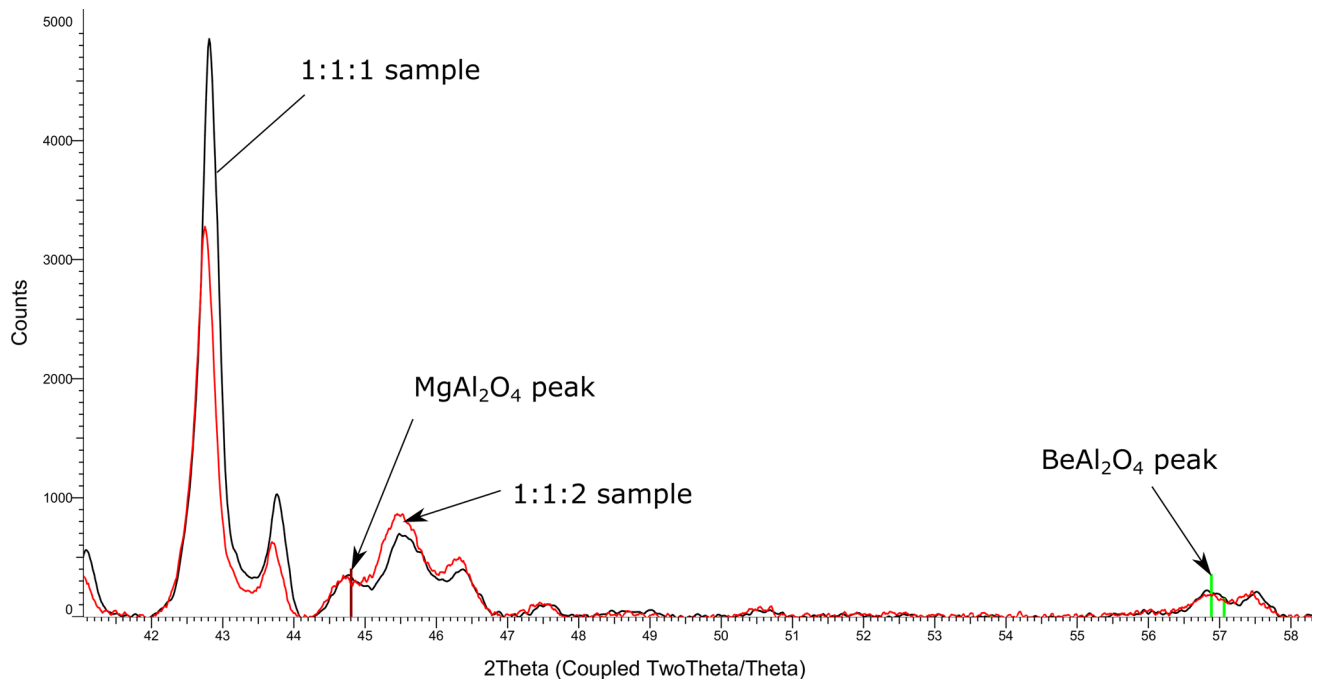
Fig. 15—A portion of the XRD patterns from oxide mixing experiments showing both the 1:1:1 and 1:1:2 mixing ratios. Both $BeAl_2O_4$ and $MgAl_2O_4$ are seen to form in similar amounts (same peak intensity) where the binary oxides show different amounts. Unlabeled peaks correspond to the binary MgO, BeO, or Al_2O_3 oxides phases.

1. Native MgO oxide layer due to oxidation at room temperature and heating up to molten state. Be is homogeneously distributed throughout the melt

2. Mg is transported from the bulk through the native oxide layer and forms a new granular oxide layer. Be is transported to the oxide-metal interface and reacts with the native oxide layer to form BeO.

3. BeO layer creates a barrier between the melt and native oxide layer. Mg and Al will diffuse across the BeO layer.

4. Due to the low free Mg content in the native oxide layer the $MgAl_2O_4$ phase becomes stable and forms. Additionally the $BeAl_2O_4$ phase is stable due to the low amount of free Be and forms. Breakaway oxidation is delayed as the formation of the $MgAl_2O_4$ spinel phase, which is key to breakaway oxidation, is controlled by Al diffusion through BeO.
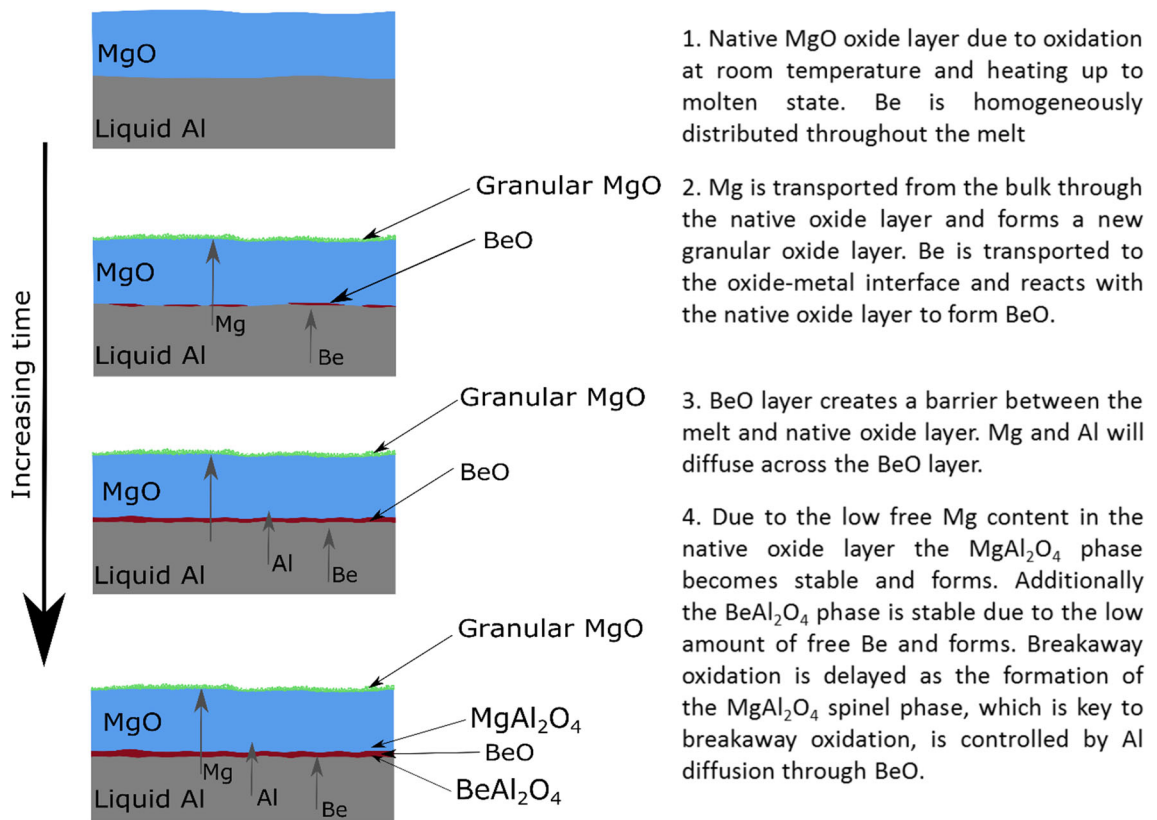
Fig. 16—Proposed mechanism behind the protective effect of Be on Mg-containing Al melts.

For the oxide stability tests, the similar heights of the $BeAl_2O_4$ and $MgAl_2O_4$ peaks for both oxide mixing ratios indicates a similar amount of the phases in both samples regardless of the initial mixing ratio. This means that both the $BeAl_2O_4$ and $MgAl_2O_4$ spinel phases exist and can form simultaneously in a system containing Mg, Be, Al, and O.

Based on the results and discussion above the proposed reaction and protection mechanism of an Al-Mg alloy containing Be is given in Figure 16. The proposed steps in the oxidation are:

1. The starting point of this model is taken as a liquid Al-Mg alloy with a layer of MgO. The MgO layer will form as a result of oxidation at room temperature, heating, and melting. While BeO is a more stable oxide than MgO, the initial oxide layer is found to be MgO as the activity of Mg is significantly higher than the Be at ppm levels. Any Be present on the surface will have reacted to form BeO; however, given the small amounts of Be that would be present at the surface, any BeO formed is neglected at this stage.

2. As metallic Be interacts with the MgO layer, it will react to form BeO and Mg per Eq. [2] rather than the direct oxidation with oxygen through Eq. [3]. Due to the rapid diffusion of Be in the liquid alloy, an elevated concentration of Be compared with the bulk alloy will form resulting in a higher Be activity at the oxide–metal interface. This higher Be activity will help to drive the oxidation of Be to BeO. The diffusion of Be to the oxide–metal interface will happen rapidly given the small atomic radius of the Be atom as the diffusion coefficient is inversely proportional to the atomic radius. With the atomic radius of Be at 1.12 Å compared to 1.60 Å for Mg and 1.43 Å for Al, the Be should diffuse rapidly through the liquid Al allowing for significant and rapid Be concentration at the oxide–metal interface.[12]

$$MgO + Be = BeO + Mg \qquad [2]$$

$$Be + O = BeO \qquad [3]$$
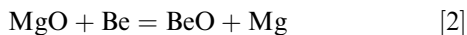
3. As holding time in the liquid state increases, a continuous BeO layer will begin to form at the oxide–metal interface since the primary source of oxygen for the oxidation of Be is the MgO layer. The areas on the BeO layers that are the thinnest will have the highest access to oxygen and see the most growth. This results in a relatively uniform layer of BeO covering the entire oxide–metal interface. While this BeO layer is forming, Mg from the metal and as a byproduct from Be oxidation, will continue to diffuse outward and cause the granular oxidation on the surface of the oxide.

Once the BeO layer has formed and covered the entire oxide–metal interface, a barrier between the metal and oxide has been established, and diffusion across this BeO layer is required for any further oxidation of Be, Mg, or Al to occur.

For the 100 ppm Be samples, the BeO layer ranges from 15 to 50 nm thick and an average of around 40 nm after 6 hours at 700 °C. The layer for the 2 ppm samples could not be observed on the FIB, and therefore must be at least one order of magnitude thinner. If the entire Be content in the sample was oxidized to BeO, the thickness of the layer would be approximately 250 nm for the 100 ppm sample and 5 nm for the 2 ppm sample based on the sample size used. Based on the average BeO layer thickness, 16 pct of the Be in the 100 ppm sample was oxidized at 700 °C indicating a strong tendency to segregate to the oxide layer. Regardless of the thickness of this layer, it must act as an effective barrier to the diffusion.

4. The MgO layer will be nearly free of metallic Mg and Al, and thus, a diffusion gradient will be established and flux of these elements across the BeO layer will develop. The diffusion coefficients of Mg and Al through the hexagonal BeO layer are not available at this momemt, rendering the calculations of the actual rates of Mg and Al diffusion across this layer as not possible. The smaller atomic size of Be compared with Mg should significantly reduce the ability of Mg to diffuse outward through the BeO layer compared with the initial MgO layer. In addition, the MgO layer is generally considered to be a noncontinuous layer and acts as a poor transport barrier. The smaller diameter and higher concentration of Al compared with Mg means Al will have a higher flux across the BeO layer than Mg. Given the limited supply of both Mg and Be to the system, it is assumed that the $MgAl_2O_4$ and $BeAl_2O_4$ phases will be the most stable and form via Eqs. [1] and [4]. The oxide-stability experiments show that both these phases can exist under nonequilibrium conditions. It is well established that the $MgAl_2O_4$ phase only becomes stable after the metallic Mg activity has dropped below 0.023. This has not been shown for the $BeAl_2O_4$ spinel, but given the similar oxidation characteristics, it is assumed the same is also true for the $BeAl_2O_4$ phase.

$$4BeO + 2Al = BeAl_2O_4 + 3Be \qquad [4]$$
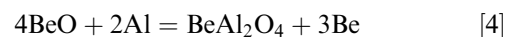
Breakaway oxidation is delayed as the formation of the $MgAl_2O_4$ phase is now diffusion controlled. Before the BeO layer formed, the MgO was in direct contact with Al. This allowed rapid transformation of MgO to $MgAl_2O_4$. The BeO layer now acts as a barrier separating the Al from the MgO causing the $MgAl_2O_4$ reaction rate to become tied to the diffusion of Al across BeO.

Based on the proposed mechanism above suggestions for alternative alloying additions can be made. An alternate element should react to form a diffusion barrier at the oxide metal interface. To encourage the formation of this layer an alternative element would need to have a strong tendency to segregate to the oxide–metal interface and readily react to from a protective layer. From this several candidates can be proposed, such as other group 2 elements or rare earth elements. In regards to the group 2 elements, Sr seems to

be the obvious candidate as it oxidizes preferentially to magnesium. Previous studies on the effects of Sr on the oxidation have shown mixed results with its effectiveness for inhibiting oxidation.[13,14] Rare earth elements stand out as a potential alternative as they are surface active and will readily react. Yttrium has seen usage as an alloying element to reduce the oxidation of solid Mg alloys at 500 °C and may prove effective in controlling the oxidation of liquid AlMg alloys.[15–17] The effect of both Sr and rare earth elements on the oxidation will be the subject of further research.

V. CONCLUSION

Industrial (2 ppm Be) and model (100 ppm Be) Al-Mg alloys have been oxidized in air at temperatures between 550 °C and 750 °C in order to establish the mechanism by which Be provides oxidation protection to Al-Mg alloys. Based on the results from FIB and XPS studies of the oxidized surface, a protection mechanism has been proposed, and the following conclusions have been made:

- On samples below the melting point, Be forms as $BeO-Al_2O_3$ growths on the surface in combination with MgO.
- The composition of these growths does not correspond to a $BeAl_2O_4$ phase, but rather a $BeO-BeAl_2O_4$ phase. The ratio of Al oxide:Be oxide increases with depth in the growth.
- On samples below the melting point, the surface growths form predominantly in areas most prone to oxidation such as grain boundaries, and thus act to slow the oxidation as a network of MgO continues to form and grow around the $BeO-BeAl_2O_4$ growths.
- On molten samples, the BeO forms a uniform layer of 15 to 50 nm thickness under an initial MgO surface layer for a sample with 100 ppm Be and 4.5 pct Mg.
- This BeO layer acts as a barrier to Mg and Al diffusion into the oxide thus slowing MgO and $MgAl_2O_4$ formation.

In addition, the stability of the $MgO-BeO-Al_2O_3$ ternary oxide system and the formation of $MgAl_2O_4$ or $BeAl_2O_4$ were studied along with the metal–oxide reaction of an Al drop with trace Be amounts on Al_2O_3 and MgO, and experiments have been carried out where the following were found:

- Both $MgAl_2O_4$ and $BeAl_2O_4$ will form in the ternary $MgO-BeO-Al_2O_3$ oxide system after a holding time of 7 hours at 1100 °C.
- Addition, of 30 and 60 ppm of Be to Al will have negligible impact on the wetting angle on a Al_2O_3 substrate. The same alloys on an MgO substrate will rapidly react to form an $MgAl_2O_4$ reaction layer.

REFERENCES

1. S. Balicki: *Prace Inst.*, 1958, vol. 10, pp. 208–13.
2. W. Thiele: *Aluminium*, 1962, vol. 38, pp. 780–86.
3. C. Cochran, D. Belitskus, and D. Kinosz: *Metall. Mater. Trans. B*, 1977, vol. 8B, pp. 323–32.
4. G. Sigworth: *Best Practices in Aluminum Metalcasting*, American Foundry Society, Schaumburg, IL, 2014.
5. K. Surla, F. Valdiveso, M. Pijolat, M. Soustelle, and M. Prin: *Solid State Ionics*, 2001, vol. 143, pp. 355–65.
6. S. Bao: Ph.D. Thesis, NTNU, Trondheim, Norway, 2011, pp. 4–80.
7. N. Smith: *Light Metals 2017*, TMS2017, San Deigo, pp. 1465–74.
8. I. Haginoya and T. Fukusako: *Trans. JIM*, 1983, vol. 24 (9), pp. 613–19.
9. K. Wefers: *Aluminum*, 1981, vol. 57, pp. 722–26.
10. N. Smith: *Light Metals*, TMS2018, Phoenix, 2018, pp. 913–19.
11. M. Syvertsen: *Light Metals*, TMS2017, San Diego, 2015, pp. 1451–55.
12. T. Engh: *Principles of Metal Refining*, 1st ed., Oxford University Press, New York, NY, 1992, pp. 114–17.
13. O. Ozdemir, E. Gruzleski, and A. Drew: *Oxid. Metals*, 2009, vol. 72, pp. 241–57.
14. S. Miresmaeili: *Metal*, 2005, vol. 2005, pp. 223–31.
15. X. Wang, X. Zeng, G. Wu, and S. Yao: *Appl. Surf. Sci.*, 2006, vol. 253, pp. 2437–42.
16. X. Wang, X. Zeng, G. Wu, S. Yao, and Y. Lai: *Appl. Surf. Sci.*, 2007, vol. 253, pp. 3574–80.
17. X. Wang, X. Zeng, G. Wu, and S. Yao: *Mater. Lett.*, 2007, vol. 61, pp. 968–70.